

Two - plasmon decay as a reason for anomalous absorption and backscattering in second harmonic ECRH experiments

A.Yu. Popov, E.Z. Gusakov

Ioffe Institute, St. Petersburg, Russia

1. Introduction. Electron cyclotron resonance heating (ECRH) at power level of up to 1 MW in a single microwave beam is used nowadays in tokamak and stellarator experiments and considered for application in ITER for neoclassical tearing mode control. The analysis of parametric decay instabilities (PDIs) potentially dangerous for mm-waves at ECR frequencies was performed more than a couple of decades ago [1] under the assumption of a monotonous background density profile. It revealed the typical microwave power thresholds in the range much higher than 1 MW and predicted the nonlinear effects to be not important in the ECRH experiments utilizing gyrotrons. However, during the last decade many experiments, which were carried out in the presence of a non-monotonous density profile, originated due to the magnetic island or the density pump-out effect, have demonstrated excitation of anomalous phenomena in the ECRH experiments at Textor, TCV, TJ-II, ASDEX-U and FTU. The clearest evidence of nonlinear effect has been obtained at the Textor tokamak [2, 3] where strong backscattering signal down-shifted in frequency by approximately 1 GHz and synchronized to the MHD mode rotation was observed in the 200 – 600 kW power level 2nd harmonic X mode ECRH experiment.

In the present paper we introduce a model taking into account, as distinct from the standard theory [1], the presence of a non-monotonous density profile in the magnetic island [4] and interpret the generation of the backscattering signal as a secondary nonlinear process, which accompanies a primary low – threshold two–upper hybrid (UH) – plasmon PDI of the X wave [5]. The power threshold of the primary absolute PDI appears to be drastically smaller than predicted by [1] due to the UH waves trapping in a vicinity of the O-point of the magnetic island where the UH frequency is close to one-half the pump frequency. The PDI is excited during each passage of the island across the ECRH beam.

The primary PDI enhancing the UH wave fluctuations from the thermal noise level is saturated in our model due to a secondary low-threshold decay of the daughter UH wave leading to excitation of the secondary UH wave down-shifted in frequency and the low hybrid (LH) wave. The threshold of this cascading process can be easily overcome when the secondary UH wave is trapped in the radial direction due to a local maximum of the density profile. We derived and then solved numerically a set of equations describing the cascading process. The results of numerical modelling are compared to the analytical estimations of the growth rates of the primary and secondary parametric decays and the saturation level. It is demonstrated that for the Textor conditions [2, 3] approximately 20% of the pump wave power can be anomalously absorbed by the decay waves.

The generation of the backscattering signal is explained in terms of the nonlinear coupling of different daughter UH waves. This mechanism appears capable of reproducing the fine details of both the frequency spectrum and the absolute value of the observed backscattering signal [2, 3]. The saturation of exponential growth of the daughter waves amplitudes and the transition to a quasi-stationary regime of the PDI are shown below to

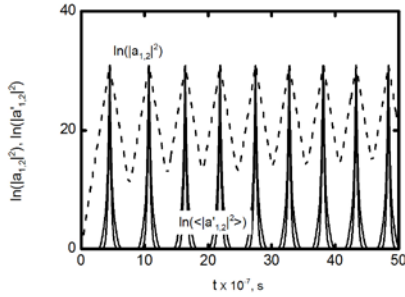


Fig. 1: Evolution of the number of the primary (dashed curve) and secondary (solid curve) plasmons in the presence of a homogeneous pump $a_0 = \text{const.}$

magnetic field $\mathbf{H} = H\mathbf{e}_z$ in the density inhomogeneity direction along a unit vector \mathbf{e}_x . The basic set of the equations, describing the pump X wave decay into a couple of the electrostatic UH plasmons trapped in the radial direction and propagating in opposite directions, as well as the decay of the second primary daughter plasmon to the radially trapped secondary UH plasmon and the low hybrid (LH) plasmon, possessing frequencies satisfying decay conditions $\omega_0 = \omega_1 + \omega_2$, $\omega_2 = \omega'_1 + \omega'_2$ reads as [6]

$$\begin{aligned} \frac{\partial a_1}{\partial t} + u_{1y} \frac{\partial a_1}{\partial y} - i\Lambda_{1z} \frac{\partial^2 a_1}{\partial z^2} &= \nu_0 a_0(y, z) a_2, \quad \frac{\partial a_2}{\partial t} - u_{2y} \frac{\partial a_2}{\partial y} + i\Lambda_{2z} \frac{\partial^2 a_2}{\partial z^2} = \nu_0^* a_0^*(y, z) a_1 \\ \frac{\partial a'_1}{\partial t} + u'_{1y} \frac{\partial a'_1}{\partial y} + i\Lambda'_{1y} \frac{\partial^2 a'_1}{\partial y^2} - u'_{1z} \frac{\partial a'_1}{\partial z} &= \nu_1^* a_2 a'_1, \quad \frac{\partial a'_2}{\partial t} - i\Lambda'_{2y} \frac{\partial^2 a'_2}{\partial y^2} + u'_{2z} \frac{\partial a'_2}{\partial z} = \nu_1 a_2^* a'_1 \end{aligned} \quad (1)$$

where u_{1y} , u_{2y} , u'_{1y} are the poloidal group velocities averaged over the UH plasmons radial localization areas and describing their convective energy loss from the decay region in the poloidal direction, Λ_{1z} , Λ_{2z} , Λ'_{1y} are the coefficients averaged over the UH plasmons radial localization areas and describing their diffraction energy loss along the magnetic field, u'_{2z} and Λ'_{2y} describe the toroidal convective and poloidal diffractive energy loss of the secondary LH wave, ν_0 and ν_1 describe the parametric coupling of the two primary UH plasmons and the primary and secondary UH plasmons, respectively, $|a_0|^2$, $|a_{1,2}|^2$, $|a'_{1,2}|^2$ are the number of photons, primary and secondary plasmons. We solve (1) numerically in a 2D box $2y_B \times 2z_B$ and impose the boundary conditions in a way to take full account of the 2D translational symmetry over the poloidal and toroidal coordinates which allows improving stability of the numerical scheme. As initial conditions for decay wave amplitudes we take the thermal noise spectral power density integrated over the wave number space region for plasmons participating in the PDI

occur just after the one-stage cascade. Taking into account the multiple-stage cascade does not change the estimation of the saturation level derived within the one-stage cascade model.

2. Equations describing the X-mode pump PDI cascade.

To elucidate the physics of the X-mode pump PDI, we consider the most simple but nevertheless relevant to the experiment three-wave resonance interaction model and analyse the behaviour of the pump X wave propagating inwards plasma in the tokamak mid-plane almost perpendicular to the

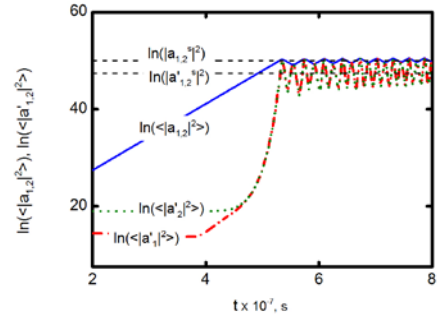


Fig. 2: The number of the primary plasmons (solid blue curves) and secondary UH (dash-dotted red curve) and LH (shot-dashed green curve) plasmons. The horizontal dashed lines correspond to the saturation level (2) of the primary (upper line) and secondary daughter plasmons (lower line).

As initial conditions for decay wave amplitudes we take the thermal noise spectral power density integrated over the wave number space region for plasmons participating in the PDI

$$|a_{1,2}|^2(0, \mathbf{r}) = T_e / (\omega_{1,2} \pi w^2), \quad |a'_{1,2}|^2(0, \mathbf{r}) = T_e / (\omega'_{1,2} \pi w^2) \quad (w = 1\text{cm} \text{ is the pump beam radius}).$$

The coefficients of the system (1) are constant.

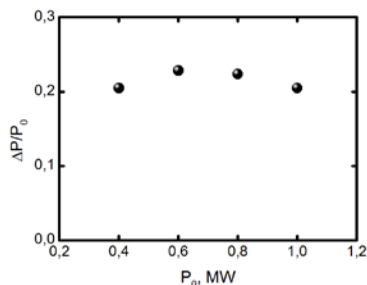


Fig. 3: Dependence $\Delta P / P_0$ (ΔP is the power which the daughter waves gain due to the PDI (3)) on the pump power P_0 for the typical Textor conditions.

demonstrated at the beginning of computing. As soon as the number of the primary plasmons turns to be large enough to exceed the threshold of the secondary decay, the number of the secondary plasmons starts to grow as well. When the secondary PDI power threshold is exceeded significantly, the temporal gain coefficient can be estimated as $2\Gamma_s(t) \approx 2|\nu_1| \sqrt{\langle |a_2(t)|^2 \rangle} / (|\nu_0| |a_0|)$. Keeping in mind the last estimation of the temporal gain coefficient along with the steady balance between the fractions of power gained by the primary UH wave from the pump X wave and by the secondary UH wave from the primary one, we get, eventually, the estimate of the saturation level of the primary and secondary plasmons

$$|a_2^s|^2 = \left[\frac{|\nu_0|}{|\nu_1|} |a_0| \ln \left(\frac{|\nu_0|}{|\nu_1|} \frac{|a_0|}{\sqrt{2} a'_1(0)} \right) \right]^2, \quad |a_1'^s|^2 = |a_0|^2 \frac{|\nu_0|^2}{|\nu_1|^2} \ln \left(\frac{1}{\sqrt{2}} \frac{|\nu_0|}{|\nu_1|} \frac{|a_0|}{a'_1(0)} \right) \quad (2)$$

These estimations (2) shown in fig. 2 are in a reasonable agreement with the results of numerical modeling. As we can see, in the quasi-stationary regime weak oscillations of the number of the daughter plasmons around the corresponding saturation level occur. Nevertheless, these oscillations, especially in the case of the primary plasmons, are much weaker than those in the case of the homogeneous pump (compare to fig. 1). Then, we get numerically the power which the daughter waves gain

$$\Delta P = \frac{\partial}{\partial t} \int_S dy dz \left[\omega_1 |a_1(y, z, t)|^2 + \omega_2 |a_2(y, z, t)|^2 + \omega'_1 |a'_1(y, z, t)|^2 + \omega'_2 |a'_2(y, z, t)|^2 \right] \quad (3)$$

In fig. 3 the dependence of the relative power loss of the pump X wave on the pump power for the typical Textor tokamak conditions is shown. It demonstrates that for the Textor conditions [2,3] up to 22% of the pump wave power can be anomalously absorbed by the decay waves.

3. Comparison to the experimental observations [3]. The experimental observations of strong anomalous backscattering of mm-waves in Textor plasmas were achieved with the use of the collective Thomson scattering (CTS) technique [3] a scheme of which is

We start with analysis of a homogeneous pump $a_0 = \text{const}$. In this case numerical solution of system (1) shown in fig. 1, demonstrates oscillatory regime of the daughter waves interaction.

In the case of the realistic finite-size pump beam ($P_0 = 600\text{kW}$) the results of numerical modeling for the typical Textor experimental parameters are shown in fig. 2 where the temporal dependencies $\ln[\langle |a_{1,2}(t)|^2 \rangle]$ (solid blue curves) and $\ln[\langle |a'_{1,2}(t)|^2 \rangle]$ (dash-dotted red and shot-dashed green curves) are depicted (The averaging is defined as $\langle |a_{1,2}(t)|^2 \rangle = \int_{-y_B}^{y_B} \int_{-z_B}^{z_B} dy dz |a_{1,2}(y, z, t)|^2 / (2y_B 2z_B)$). The exponential

growth of the number of the primary plasmons is

demonstrated at the beginning of computing. As soon as the number of the primary plasmons turns to be large enough to exceed the threshold of the secondary decay, the number of the secondary plasmons starts to grow as well. When the secondary PDI power threshold is exceeded significantly, the temporal gain coefficient can be estimated as $2\Gamma_s(t) \approx 2|\nu_1| \sqrt{\langle |a_2(t)|^2 \rangle} / (|\nu_0| |a_0|)$. Keeping in mind the last estimation of the temporal gain coefficient along with the steady balance between the fractions of power gained by the primary UH wave from the pump X wave and by the secondary UH wave from the primary one, we get, eventually, the estimate of the saturation level of the primary and secondary plasmons

$$|a_2^s|^2 = \left[\frac{|\nu_0|}{|\nu_1|} |a_0| \ln \left(\frac{|\nu_0|}{|\nu_1|} \frac{|a_0|}{\sqrt{2} a'_1(0)} \right) \right]^2, \quad |a_1'^s|^2 = |a_0|^2 \frac{|\nu_0|^2}{|\nu_1|^2} \ln \left(\frac{1}{\sqrt{2}} \frac{|\nu_0|}{|\nu_1|} \frac{|a_0|}{a'_1(0)} \right) \quad (2)$$

These estimations (2) shown in fig. 2 are in a reasonable agreement with the results of numerical modeling. As we can see, in the quasi-stationary regime weak oscillations of the number of the daughter plasmons around the corresponding saturation level occur. Nevertheless, these oscillations, especially in the case of the primary plasmons, are much weaker than those in the case of the homogeneous pump (compare to fig. 1). Then, we get numerically the power which the daughter waves gain

$$\Delta P = \frac{\partial}{\partial t} \int_S dy dz \left[\omega_1 |a_1(y, z, t)|^2 + \omega_2 |a_2(y, z, t)|^2 + \omega'_1 |a'_1(y, z, t)|^2 + \omega'_2 |a'_2(y, z, t)|^2 \right] \quad (3)$$

In fig. 3 the dependence of the relative power loss of the pump X wave on the pump power for the typical Textor tokamak conditions is shown. It demonstrates that for the Textor conditions [2,3] up to 22% of the pump wave power can be anomalously absorbed by the decay waves.

3. Comparison to the experimental observations [3]. The experimental observations of strong anomalous backscattering of mm-waves in Textor plasmas were achieved with the use of the collective Thomson scattering (CTS) technique [3] a scheme of which is

sketched out in fig. 4. The backscattering signal collected by the receiving CTS antenna located around 20 cm above the gyrotron launcher can be explained in terms of the nonlinear coupling of the primary ($\omega_l/2\pi = 69.82\text{GHz}$) and secondary ($\omega'_l/2\pi = 69.22\text{GHz}$) UH waves leading to excitation of the X wave propagating outwards. The frequency of the latter, $\omega_a/2\pi = (\omega'_l + \omega_l)/2\pi = 139.04\text{GHz}$, corresponds to the first down-shifted spectral line observed experimentally (fig. 9 in [3]).

Utilizing the approach based on the reciprocity theorem [7], we get the power of a signal collected by the microwave antenna

$$p_s(\omega_a) = \frac{\alpha}{c\pi w_a^2} \frac{W_1 W'_1}{w_H} \quad (4)$$

where α is the dimensionless geometrical factor, $w_a \approx 1.5\text{cm}$ is a radius of the horn of the receiving antenna, W_1 , W'_1 are energies of the radially trapped primary and secondary UH plasmons calculated numerically, and $w_H = H^2/4\pi$ is energy density of the external magnetic field. For the parameters of the ECRH experiments at Textor (see captions for fig. 1) in which the strong anomalous backscattering of the X-mode pump was observed the estimate of the anomalously backscattered X wave spectral line intensity (4) is $p_s(\omega_a)/\Delta\nu = 0.602\text{MeV}$ with $\Delta\nu \approx 0.2\text{GHz}$ being experimentally measured spectrum line-width. This calculated value is of the order of the spectral power density value provided by the CTS measurements $p_s(\omega_a)/\Delta\nu \approx 1\text{MeV}$ (see figs. 9, 11 in [3]).

4. Conclusions. Summarizing, we can conclude that the proposed mechanism of the backscattering signal generation based on the low threshold excitation in the magnetic island of the two-plasmon PDI and its cascading saturation appears capable of reproducing both the fine details of the frequency spectrum and absolute level of the observed anomalous backscattering signal [3]. It should be stressed that this mechanism predicts substantial anomalous absorption of the pump. In particular, up to 22% of the pump power is anomalously absorbed by the decay waves for the TEXTOR experimental parameters.

The computations were performed at facilities of USD “Globus-M”. Partial financial support of RFBR grant 13-02-00683, BRFBR-RFBR grant 14-02-90003 and RF MES (Agreement 14.619.21.0001, id RFMEFI61914X0001) is acknowledged.

- [1] M. Porkolab, B.I. Cohen 1988 *Nucl. Fusion* **28** 239
- [2] E. Westerhof, S. Nielsen, J. W. Oosterbeek et al. 2009 *Phys. Rev. Lett.* **103** 125001
- [3] S.K. Nielsen, M. Salewski, E. Westerhof et al. 2013 *Plasma Phys. Control. Fusion* **55** 115003
- [4] M.Yu. Kantor 2009 *Plasma Phys. Control. Fusion* **51** 055002
- [5] A.Yu. Popov, E.Z. Gusakov 2015 *Plasma Phys. Control. Fusion* **57** 025022
- [6] A.Yu. Popov, E.Z. Gusakov 2015 *JETP* **121** to be published in vol 1
- [7] A D Piliya, A Yu Popov 2002 *Plasma Phys. Control. Fusion* **44** 467

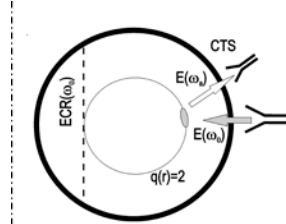


Fig. 4: Tokamak cross-section illustrating the Textor experimental setup [3].